

# Rigid-Rod Polyesters with Flexible Side Chains Based on 1,4-Dialkyl Esters of Pyromellitic Acid. 1

Brian R. Harkness and Junji Watanabe\*

Department of Polymer Chemistry, Tokyo Institute of Technology, Ookayama, Meguro-ku, Tokyo 152, Japan

Received April 17, 1991; Revised Manuscript Received September 9, 1991

**ABSTRACT:** The 1,4-di-(1-tetradecyl ester) of 1,2,4,5-benzenetetracarboxylic acid has been prepared and copolymerized with hydroquinone and 4,4'-biphenol. These polymers, designated as H-C14 and B-C14, respectively, have been observed to form thermotropic liquid crystalline phases. An X-ray examination of these mesophases has revealed that they adopt layered structures. B-C14 displays two distinct layerlike modifications which depend on temperature, whereas the H-C14 mesophase assumes a single layered structure that has a greater degree of order than the B-C14 mesophases. The structural characteristics of these mesophases are given according to the X-ray data collected for oriented specimens.

## Introduction

There have been many reports in the literature concerning the preparation and liquid crystalline properties of rigid-rod polyesters with flexible alkyl side chains.<sup>1-9</sup> The object of these studies has been to develop liquid crystalline materials with lower melting temperatures and greater solubilities than the simple rigid-rod polyesters that lack side groups. As a result of these investigations, not only have these goals been attained but also some very interesting liquid crystalline phases have been observed.

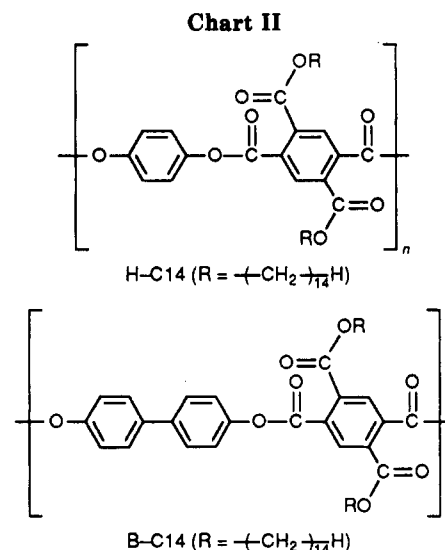
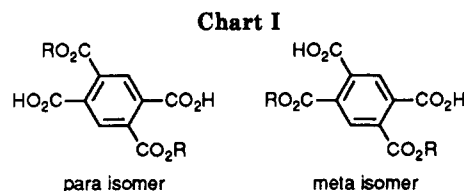
There has recently been a report in the patent literature<sup>10</sup> concerning the preparation and purification of long-chain dialkyl esters of 1,2,4,5-benzenetetracarboxylic acid (pyromellitic acid), with the general structures shown in Chart I. These materials can be prepared as a mixture by the reaction of pyromellitic dianhydride with a long-chain alcohol ( $10 \leq n \leq 30$ , where  $n$  denotes the number of carbon atoms in the chain) and then separated according to their different solubilities in halogenated organic solvents. Isolation of the pure para isomer would yield a monomer from which several new rigid-rod polyesters with long  $n$ -alkyl side chains could be derived.

In this preliminary report we will discuss the liquid crystalline properties of two novel polyesters derived from the para isomer with  $n$ -tetradecyl side groups. These new polyesters were prepared as comonomers with hydroquinone and 4,4'-biphenol and are designated as H-C14 and B-C14, respectively (Chart II).

## Experimental Section

**Materials and Methods.** Tetrahydrofuran (THF) and toluene were distilled from  $\text{LiAlH}_4$  prior to use. Triethylamine was distilled from  $\text{NaH}$ . Pyromellitic dianhydride (1,2,4,5-benzenetetracarboxylic dianhydride; Tokyo Chemical) and 1-tetradecanol (Tokyo Chemical) were used without further purification. Hydroquinone and 4,4'-biphenol (Mitsubishi Petrochemical) were obtained with a purity of 99.9%.

<sup>1</sup>H NMR spectra were obtained with a JEOL FX90Q spectrometer at a frequency of 90 MHz. DSC measurements were performed with a Perkin-Elmer DSC-II calorimeter at a scanning rate of 10 °C/min. Wide-angle X-ray diffraction patterns of the polymers were recorded with a flat-plate camera mounted to a Rigaku-Denki X-ray generator emitting Ni-filtered  $\text{Cu K}\alpha$  radiation. The temperature of the samples was controlled by placing the samples in a Mettler FP-80 hot stage mounted in the beam path. The film to specimen distance was determined by calibration with silicon powder. Optical microscopic observations of the liquid crystalline textures were made with an Olympus BH-2 polarizing microscope equipped with a Mettler FP-80 hot stage.



**1,4-Di-(1-tetradecyl ester) of 1,2,4,5-Benzenetetracarboxylic Acid.** Into a 500-mL round-bottomed flask, equipped with a magnetic stirbar, was placed 20 g (0.092 mol) of pyromellitic dianhydride and 39.3 g (2 mol equiv) of 1-tetradecanol. The flask was sealed with a drying tube, and the contents were slowly heated to 150 °C with an oil bath. After stirring for 45 min at 150 °C, the molten product was cooled, resulting in the crystallization of the meta and para dialkyl esters of pyromellitic acid. To the flask was then added 400 mL of acetone, and the mixture was slowly stirred for approximately 12 h. Filtration of the remaining solid material yielded the pure para dialkyl ester product. The meta dialkyl ester (which also contained a small amount of the para isomer) could be recovered by evaporation of the acetone extract. In a second purification step, the para dialkyl ester was washed with 200 mL of methylene chloride for about 3 h. Filtration and drying of the product gave 18.4 g (31% yield) of the para dialkyl ester.

**Diacid Chloride of the 1,4-Di-(1-tetradecyl ester) of 1,2,4,5-Benzenetetracarboxylic Acid.** Into a 50-mL round-bottomed flask, equipped with a magnetic stirbar, was placed 6.83 g (0.0106 mol) of the 1,4-di-(1-tetradecyl ester), 20 mL of THF, and approximately 4 mol equiv of thionyl chloride. The

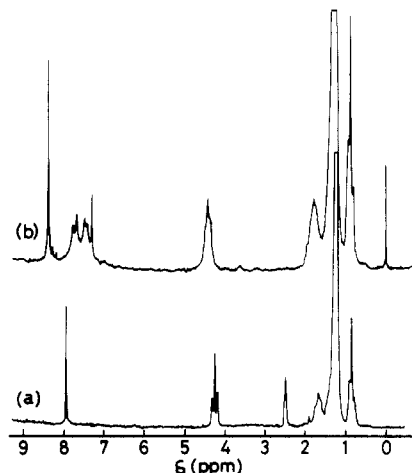


Figure 1.  $^1\text{H}$  NMR spectra of (a) the *p*-di-(1-tetradecyl ester) of pyromellitic acid and (b) the B-C14 polyester as recorded in  $\text{DMSO}-d_6$  and  $\text{CDCl}_3$ , respectively.

flask was equipped with a condenser and heated to reflux with an oil bath heated to 80–90 °C. After refluxing for 20 min, the THF and excess thionyl chloride were removed by distillation under reduced pressure. Residual thionyl chloride was removed by adding 10 mL of toluene to the solution and continuing the distillation under vacuum. The diacid chloride product was isolated as a light yellow solid.

**Polyesters.** In a 100-mL round-bottomed flask equipped with a magnetic stirbar, 1.165 g (0.0106 mol) of hydroquinone was dissolved in 30 mL of THF and slightly more than 2 equiv of triethylamine. In a separate 50-mL flask, exactly 1 mol equiv of the diacid chloride was dissolved in 10 mL of THF. This solution was then added over a period of 1 min to the rapidly stirred hydroquinone solution. As the reaction proceeded the solution became cloudy due to the formation of triethylamine hydrochloride. In addition, there was a marked increase in solution viscosity as well as an increase in the temperature of the reaction vessel. To ensure complete transfer of the acid chloride, the 50-mL flask was rinsed with about 3 mL of THF and this was added to the reaction flask. The flask containing the polymer solution was then equipped with a condenser and drying tube and heated to reflux with an oil bath. After 30 min the polymer solution was cooled to room temperature and poured into 250 mL of methanol to yield a tan fibrous precipitate. The polymer was purified a second time by reprecipitating a THF solution into a 5-fold excess of methanol. The same procedure was used to prepare the biphenol polyester using biphenol instead of hydroquinone.

## Results and Discussion

As described in the Experimental Section, the *m*- and *p*-di-(1-tetradecyl esters) of 1,2,4,5-benzenetetracarboxylic acid can be prepared as a mixture by reacting pyromellitic dianhydride with 1-tetradecanol at 150 °C. The para isomer was easily isolated from this mixture by taking advantage of the relatively high solubility of the meta isomer in acetone and thus washing the meta isomer away from the sparingly soluble para isomer. The purity of the para isomer was determined by  $^1\text{H}$  NMR spectroscopy. Figure 1a shows the  $^1\text{H}$  NMR spectrum for the *p*-di-(1-tetradecyl ester) in  $\text{DMSO}-d_6$ . The signals in the region 0.5–2.0 ppm and at 4.2 ppm can be assigned to the aliphatic protons of the alkyl chain. The signal peak in the aromatic region at 7.9 ppm can be assigned to the two equivalent aromatic protons of the para isomer. The meta isomer shows two peaks in the aromatic region at 8.0 and 8.4 ppm ( $\text{CDCl}_3$  solvent) that can be attributed to the two non-equivalent aromatic protons.

The polyesters H-C14 and B-C14 were found to be readily soluble in halogenated solvents such as chloroform

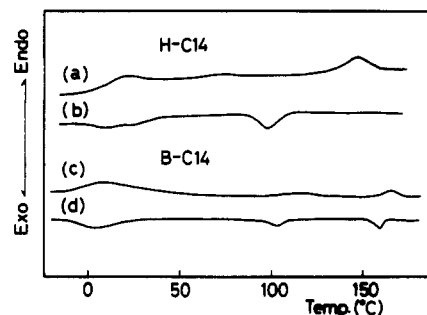


Figure 2. DSC thermograms of (a) H-C14 on heating, (b) H-C14 on cooling, (c) B-C14 on heating, and (d) B-C14 on cooling.

and also soluble in THF. The  $^1\text{H}$  NMR spectrum for the polymer B-C14 is shown in Figure 1b. The broad signals located at 0.5–2.0 ppm and at 4.4 ppm can be assigned to the alkyl side chains. In the aromatic region the broad signal located at 7.2–8.0 ppm can be assigned to the protons of the biphenyl moiety. The sharp signal at 8.4 ppm can be assigned to the two equivalent aromatic protons of the *p*-dialkyl ester component. Some negligible signals are also apparent in the aromatic region (at 8.1–8.3 ppm), and these may be attributable to end-group protons.

The inherent viscosities of the H-C14 and B-C14 polyesters were 0.23 and 0.66 dL/g, respectively, as measured in THF at 25 °C.

**Thermal Behavior and Mesophase Properties of H-C14.** The DSC scan of the H-C14 polyester, melt pressed at 160 °C, showed three transitions as the temperature was increased from –20 °C at a rate of 10 °C/min (see Figure 2). The first transition appeared around 20 °C and may originate from the melting of the side-chain crystallites. Two other transitions are observed at temperatures of 70 and 147 °C, with the latter corresponding to the liquid crystal (LC)–isotropic (Iso) phase transition of 145 °C as determined by optical microscopy. On cooling from the isotropic melt at a rate of 10 °C/min, the Iso–LC phase transition with an enthalpy of 1.20 kcal/(mol repeat unit) appeared at 98 °C, following extensive supercooling. Two additional transitions were observed around 25 and 10 °C, with the latter being associated with the crystallization of the alkyl side chains.

The phase between 70 and 147 °C, on heating, is a liquid crystalline mesophase, exhibiting fluidlike behavior between glass plates, although only a fine-grain texture can be observed by microscopy on cooling from the isotropic melt.

The X-ray diffraction pattern for a melt-drawn fiber of the H-C14 polyester at 90 °C is shown in Figure 3a, where the polymer chain axis corresponding to the fiber axis is placed in the vertical direction. The diffraction pattern exhibits a series of sharp equatorial reflections (indexed by  $h00$ ) in the small-angle region with spacings of 24.0, 12.0, 8.03, and 6.02 Å. A weak meridional streak with a spacing of approximately 12 Å also appears in the small-angle region. In addition, two wide-angle reflections are observed. The first with a spacing of approximately 4.5 Å appears as a diffuse halo, with stronger intensity on the equatorial line. The second is a sharp equatorial reflection with a spacing of 3.85 Å.

According to this X-ray data, a layered structure can be proposed for the H-C14 polyester as illustrated in Figure 3b; a similar model has been proposed for mesophases of rigid-rod polyesters with similar side-chain groups.<sup>5–9</sup> The small-angle equatorial arcs, corresponding to the maximum Bragg spacing of 24.0 Å, can be attributed to a layered structure that is formed in a direction perpendicular to

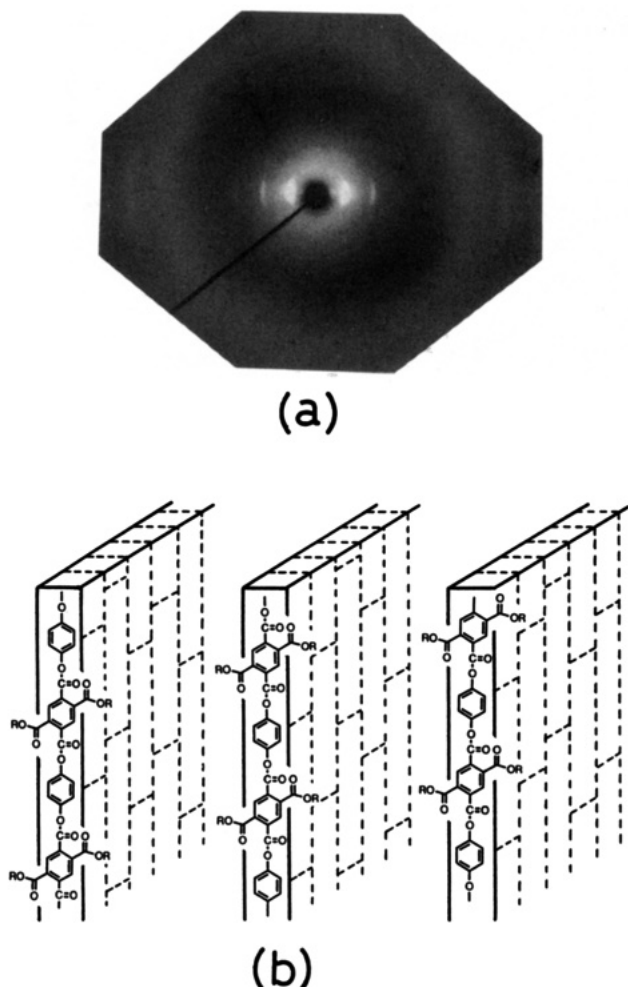


**Figure 3.** (a) X-ray photograph of a melt-spun fiber of H-C14 recorded at 90 °C (fiber axis is in the vertical direction) and (b) an illustration of the layer structure proposed for the H-C14 mesophase.

the fiber axis. Each layer is formed by a regular lateral packing of the aromatic main chains, as can be elucidated from the sharp equatorial reflection of 3.85 Å.<sup>11</sup> The main chain is in an extended conformation since the spacing of the meridional reflection, 12 Å, is in agreement with the value calculated by Erman et al.,<sup>12</sup> for a polyester with the same main-chain repeat unit. The appearance of this reflection as a streak indicates a random displacement of main chains along the chain axis as in a nematic liquid crystal. The diffuse halo with a spacing of 4.5 Å can be attributed to the highly disordered alkyl side chains that occupy the space between the layers.<sup>13</sup> The calculated density based on this structure is 1.1 g/mL and is in agreement with densities observed for mesophases of similar polyesters.<sup>6</sup>

Heating to 140 °C or cooling the fiber to room temperature did not result in any significant change in the fiber diffraction pattern. At this time we are unsure of the nature of the small transition in the DSC thermogram that appeared, on heating, at a temperature of 70 °C.

**Thermal Behavior and Mesophase Properties of B-C14.** The DSC scan of the melt-pressed B-C14 polyester also showed three small transitions on heating as shown in Figure 2. These were located at temperatures of 9, 120, and 166 °C, with the latter corresponding to the LC-Iso phase transition as determined by optical microscopy. On cooling the isotropic melt, three corresponding transitions were also apparent above -20 °C. The first with an enthalpy of 0.13 kcal/(mol repeat unit) appeared at 160 °C

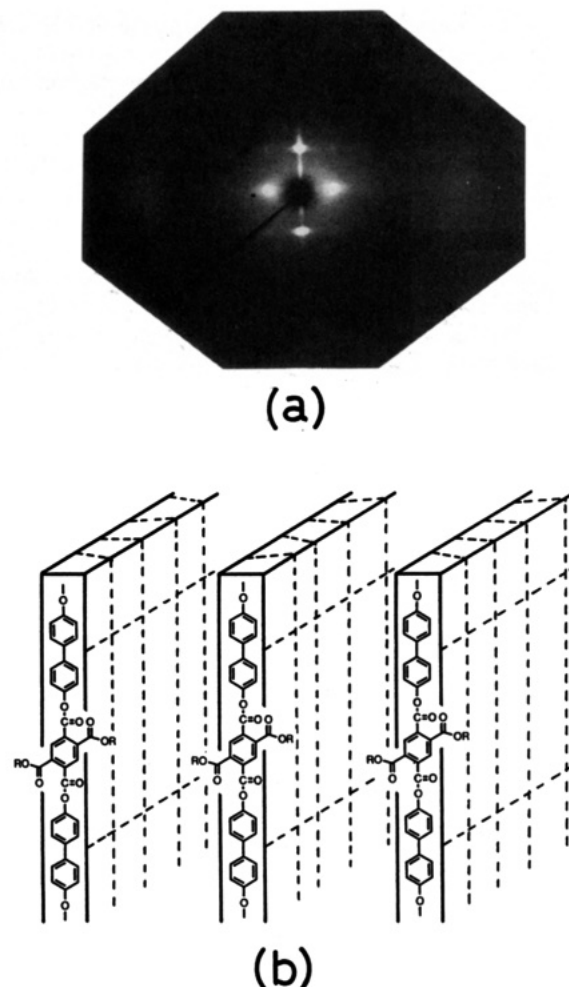


**Figure 4.** (a) X-ray photograph of a melt-spun fiber of B-C14 recorded at 70 °C (fiber axis is in the vertical direction) and (b) an illustration of the layer structure proposed for this mesophase.

and can be attributed to the Iso-LC phase transition. The second transition appeared at 103 °C, with an enthalpy of 0.10 kcal/(mol repeat unit) which is similar in magnitude to the enthalpy associated with the Iso-LC phase transition. The observation of microscopic liquid crystalline textures and sample fluidity above and below this transition indicates that it may represent the transition from one type of LC phase to another type of LC phase (LC-LC transition) as will be discussed later. The third transition that appears at around 0 °C likely results from side-chain crystallization. In comparing the DSC thermograms for the B-C14 and H-C14 polyesters, it is apparent that the enthalpy changes associated with the LC-LC and LC-Iso transitions for the B-C14 polyester are approximately one-tenth the enthalpy recorded for the LC-Iso transition for the H-C14 polyester (1.20 kcal/(mol repeat unit)). This suggests that the mesophases produced by B-C14 are less ordered than the H-C14 mesophase.

The X-ray patterns for the two B-C14 mesophases were examined at temperatures above and below the LC-LC transition temperature of 120 °C as observed on heating by DSC. Figure 4a shows the X-ray pattern for the lower temperature mesophase at 70 °C. In the small-angle region, two sharp equatorial reflections, indexed by 100 and 200 are observed with spacings of 20.5 and 10.5 Å. In addition, two sharp meridional reflections with spacings of 16.6 Å (001) and 8.30 Å (002) are evident. The 101 reflection also appears with a spacing of 12.9 Å. In the wide-angle region, two broad equatorial arcs with spacings of approximately 4.5 and 4.0 Å can be observed.

The X-ray data for the B-C14 mesophase at 70 °C is also indicative of a layered structure as illustrated in Figure 4b. The small-angle equatorial reflection, corresponding to a spacing of 20.5 Å, can be attributed to the layered spacing of the mesophase, which in this case is slightly smaller than the 24.0-Å spacing observed for the H-C14 mesophase. The appearance of only the first- and second-order reflections indicates that the layered structure is not as highly ordered as in the H-C14 mesophase. The sharp meridional reflection with a spacing of 16.6 Å is due to the repeat distance of the polymer backbone in the extended form. The intensity of this reflection as well as the appearance of the second-order reflection indicates that there is positional order along the chain axis in each layer. The appearance of the 101 reflection at 12.9 Å indicates that positional order is also maintained between neighboring layers, giving rise to a two-dimensional lattice of  $a = 20.5$  Å and  $c = 16.6$  Å. The broad reflection at 4.5 Å can be attributed to the disordered side chains occupying the space between layers. The 4.0-Å reflection likely corresponds to the lateral spacing of the main chain in each layer, and its broad appearance indicates a low degree of lateral order between the main chains. The result is a layered structure that is different from that observed for the H-C14 mesophase. The density of the low-temperature B-C14 mesophase is calculated to be 0.97 g/mL.

Heating of the B-C14 mesophase to temperatures above the LC-LC phase transition of 120 °C results in a drastic change in the X-ray pattern. Figure 5a shows the X-ray photograph taken at 130 °C. The X-ray pattern is greatly simplified, exhibiting only three distinct reflections. In the small-angle region, a broad equatorial reflection with a spacing of approximately 23.0 Å is observed. A weak meridional arc with a spacing of 15.3 Å is also visible. In the wide-angle region, only a broad arc with a spacing of approximately 4.5 Å can be distinguished. Such a pattern is very similar to that expected for a classical smectic A phase in which there is positional order along the polymer chain axis but the lateral packing of polymer chains is disordered. However, the spacing of 23.0 Å for the equatorial reflection is too large to accommodate such a smectic A structure, since in a smectic A phase, each molecule would function independently as a kinetic unit and this results in a spacing of approximately 9 Å, which corresponds to the average diameter of the molecule. Considering that the spacing of the equatorial reflection is as large as that of the lower temperature mesophase, we propose that in the higher temperature mesophase of B-C14 the main chains are still associated with each other to form a layer but the layers are packed with a greater degree of disorder. The observation of a meridional reflection with a spacing of 15.3 Å indicates that in each layer the main chains are in a somewhat extended form and still have positional order along the chain axis, although this has been reduced to some extent as compared to the lower temperature mesophase. The structure can be tentatively illustrated in Figure 5b. Finally we comment that a fine optical texture similar to a nematic texture (Figure 6) can be seen only in this mesophase.

To conclude, we have observed three modifications of the layered mesophase as illustrated in Figures 3b, 4b, and 5b. We have also shown that the type of layered mesophase formed can be dependent on temperature as shown for B-C14. In spite of these findings many questions concerning the behavior of these mesophases still remain. Presently, we are examining the liquid crystalline behavior of the C8, C10, C12, C16, and C18 derivatives so as to gain a better understanding of these layered mesophases. The

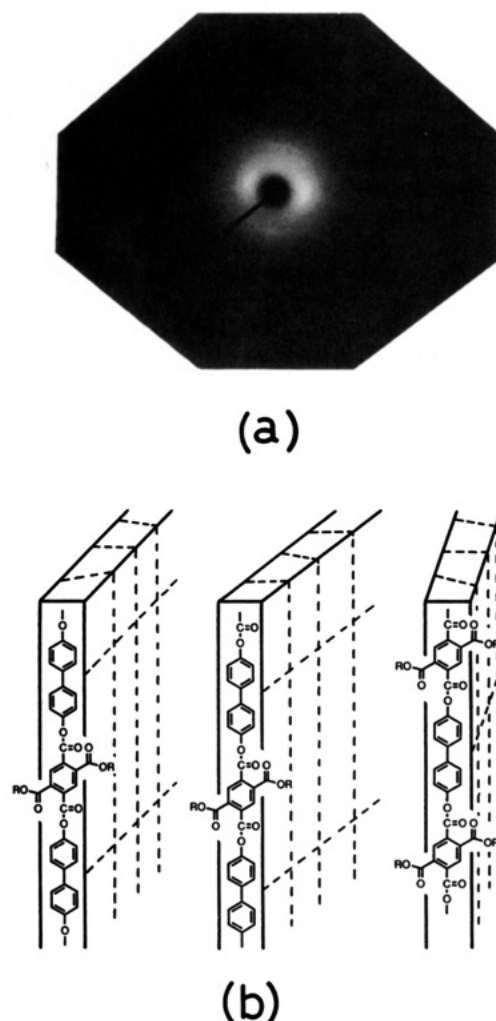


Figure 5. (a) X-ray photograph of a melt-spun fiber of B-C14 recorded at 130 °C (fiber axis is in the vertical direction) and (b) an illustration of the layer structure proposed for this mesophase.

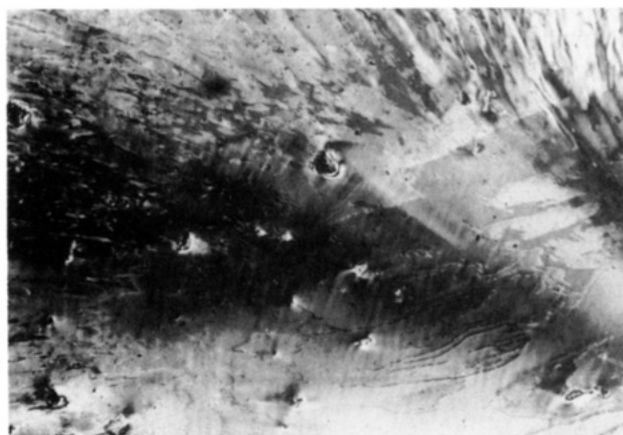


Figure 6. Texture of the B-C14 mesophase as observed under crossed polarizers at a temperature of 150 °C.

results of this investigation will be presented in a future report.

## References and Notes

- (1) Ballauff, M. *Angew. Chem., Int. Ed. Engl.* **1989**, *28*, 253.
- (2) Majnusz, J.; Catala, J. M.; Lenz, R. W. *Eur. Polym. J.* **1983**, *19*, 1043.
- (3) Krigbaum, W. R.; Hakemi, H.; Kotek, R. *Macromolecules* **1985**, *18*, 965.
- (4) Ballauff, M. *Makromol. Chem., Rapid. Commun.* **1986**, *7*, 407.

- (5) Ballauff, M.; Schmidt, G. F. *Mol. Cryst. Liq. Cryst.* **1987**, *147*, 163.
- (6) Stern, R.; Ballauff, M.; Wegner, G. *Makromol. Chem., Macromol. Symp.* **1989**, *23*, 373.
- (7) Rodriguez-Parada, J. M.; Duran, R.; Wegner, G. *Macromolecules* **1989**, *22*, 2507.
- (8) Ebert, M.; Herrmann-Schönherr, O.; Wendorff, J. H.; Ringsdorf, H.; Tschirner, P. *Liq. Cryst.* **1990**, *7*, 63.
- (9) Adam, A.; Spiess, H. W. *Makromol. Chem., Rapid Commun.* **1990**, *11*, 249.
- (10) Kamikita, M.; Awaji, H. Jpn. Kokai Tokkyo Koho JP 63,275,546 (88,275,546).
- (11) This value is substantially smaller than the main-chain distance in unsubstituted tetramers of *p*-hydroxybenzoic acid, suggesting packing of the main chains in zigzag fashion as described in ref 9.
- (12) Erman, B.; Flory, P. J.; Hummel, J. P. *Macromolecules* **1980**, *13*, 484.
- (13) Watanabe, J.; Ono, H.; Uematsu, I.; Abe, A. *Macromolecules* **1985**, *18*, 2141.